

Investigation of the asymptotic state of rotating turbulence using large-eddy simulation

By Kyle D. Squires¹, Jeffrey R. Chasnov,
Nagi N. Mansour² AND Claude Cambon³

1. Motivation and objectives

Study of turbulent flows in rotating reference frames has long been an area of considerable scientific and engineering interest. Because of its importance, the subject of turbulence in rotating reference frames has motivated over the years a large number of theoretical, experimental, and computational studies (e.g., Greenspan 1968, Bardina *et al.* 1985, Jacquin *et al.* 1990, Mansour *et al.* 1991). The bulk of these previous works has served to demonstrate that the effect of system rotation on turbulence is subtle and remains exceedingly difficult to predict.

A rotating flow of particular interest in many studies, including the present work, is examination of the effect of solid-body rotation on an initially isotropic turbulent flow. One of the principal reasons for the interest in this flow is that it represents the most basic turbulent flow whose structure is altered by system rotation but without the complicating effects introduced by mean strains or flow inhomogeneities. The assumption of statistical homogeneity considerably simplifies analysis and computation.

For an initially isotropic turbulence, it is well known that system rotation inhibits the non-linear cascade of energy from large to small scales. This effect is manifest in a reduction of the turbulence dissipation rate and associated decrease in the decay rate of turbulence kinetic energy (e.g., see Traugott 1958, Veeravalli 1991, Mansour *et al.* 1992). An issue considerably less resolved, however, is the development of a two-dimensional state in rotating homogeneous turbulence. Both computations and experiments have noted an increase in integral length scales along the rotation axis relative to those in non-rotating turbulence (Bardina *et al.* 1985, Jacquin *et al.* 1990). Increase in the integral length scales has been thought to be a prelude to a Taylor-Proudman reorganization to two-dimensional turbulence. However, it has also been shown using direct numerical simulation (DNS) of rotating isotropic turbulence (Speziale *et al.* 1987, Mansour *et al.* 1992) that in the limit of very rapid rotation, turbulence remains isotropic and three-dimensional. In fact, Mansour *et al.* (1992) showed that the evolution of rapidly rotating turbulence was accurately predicted using rapid distortion theory (RDT). Furthermore, Mansour *et al.* also

¹ University of Vermont

² NASA Ames Research Center

³ Ecole Centrale de Lyon

showed that the RDT solution violates a necessary condition for occurrence of a Taylor-Proudman reorganization.

It is worth noting that as is typically the case with DNS, the computations performed by Speziale *et al.* (1987) and Mansour *et al.* (1991,1992) were performed at low Reynolds numbers. In rotating turbulence at low Reynolds number, the effects of viscous decay progressively reduce the Rossby number and drive the flow to the RDT limit. Thus, other mechanisms for obtaining two-dimensional turbulence, e.g., through non-linear interactions which occur on a turbulence time scale, are precluded using DNS, and evolution of a two-dimensional state, therefore, requires significantly higher Reynolds numbers than can be attained using DNS.

An issue closely connected to development of two-dimensional turbulence in rotating flows is the existence of asymptotic self-similar states. The issue of self-similarity is a topic central to studies of turbulent flows (e.g., see Chasnov 1993). A similarity state is characterized by the predictability of future flow statistics from current values by a simple rescaling of the statistics; the rescaling is typically based on a dimensional invariant of the flow. Knowledge of the existence of an asymptotic similarity state allows a prediction of the ultimate statistical evolution of the flow without detailed knowledge of the complex, and not well understood, non-linear transfer processes.

Large-eddy simulation (LES) is ideally suited for examination of the long-time evolution of rotating turbulence since it circumvents the Reynolds number restriction of DNS. The drawback is, of course, that it requires use of a model to parameterize subgrid-scale stresses. However, large-scale statistics are relatively insensitive to the exact form of the model, and alternative approaches, i.e., laboratory experiments or direct simulations, are simply not feasible for examination of the long-time evolution of rotating flows.

The principal objective of the present study has thus been to examine the asymptotic state of solid-body rotation applied to an initially isotropic, high Reynolds number turbulent flow. Of particular interest has been to determine (1) the degree of two-dimensionalization and (2) the existence of asymptotic self-similar states in homogeneous rotating turbulence. As shown in §2, development of a two-dimensional state is very pronounced; much more so than observed in previous studies using DNS. It is also shown that long-time evolution of quantities such as turbulence kinetic energy and integral length scales are accurately predicted using simple scaling arguments.

2. Accomplishments

2.1 Simulation overview

In the present study, the filtered Navier-Stokes equations for an incompressible fluid were solved in a rotating reference frame:

$$\nabla \cdot \mathbf{u} = 0 \quad (1)$$

$$\frac{\partial \mathbf{u}}{\partial t} + \mathbf{u} \cdot \nabla \mathbf{u} = -\frac{1}{\rho} \nabla p + \nu_e \nabla^2 \mathbf{u} - 2\boldsymbol{\Omega} \times \mathbf{u}. \quad (2)$$

In (1) and (2), \mathbf{u} is the velocity vector, p and ρ the fluid pressure and density, respectively, and $\boldsymbol{\Omega}$ is the rotation vector. For purposes of discussion, the rotation vector is considered to act along the z or “vertical” axis, $\boldsymbol{\Omega} = (0, 0, \Omega)$. An eddy viscosity hypothesis was used to parameterize the subgrid-scale stresses. In this work, the spectral eddy viscosity of Chollet & Lesieur (1981) was modified for rotating turbulence

$$\nu_e = \nu_{e0} f(\alpha) \quad (3)$$

where ν_{e0} is the “baseline” viscosity and $f(\alpha)$ a function accounting for the reduction of ν_e by system rotation. The baseline viscosity, ν_{e0} , from Chollet & Lesieur, is

$$\nu_{e0}(k|k_m, t) = \left[0.145 + 5.01 \exp\left(\frac{-3.03k_m}{k}\right) \right] \left[\frac{E(k_m, t)}{k_m} \right]^{1/2} \quad (4)$$

where k_m is the maximum wavenumber magnitude of the simulation and $E(k, t)$ is the spherically integrated three-dimensional Fourier transform of the co-variance $\frac{1}{2} \langle u_i(\mathbf{x}, t) u_i(\mathbf{x} + \mathbf{r}, t) \rangle$ ($\langle \cdot \rangle$ denotes an ensemble or volume average). The reduction in ν_e is expressed using $f(\alpha)$

$$f(\alpha) = \frac{2[(1 + \alpha^2)^{3/2} - \alpha^3 - 1]}{3\alpha^2} \quad (5)$$

where

$$\alpha = \frac{8\Omega^2}{3E(k_m)k_m^3} \quad (6)$$

(Cambon, private communication).

The initial energy spectrum of the simulations was of the form

$$E(k, 0) = \frac{1}{2} C_s \frac{u_0^2}{k_p} \left(\frac{k}{k_p} \right)^s \exp \left[-\frac{1}{2} s \left(\frac{k}{k_p} \right)^2 \right] \quad (7)$$

where s is equal to 2 or 4, C_s is given by

$$C_s = \sqrt{\frac{2}{\pi}} \frac{s^{\frac{1}{2}(s+1)}}{1 \cdot 3 \cdot \dots \cdot (s-1)} \quad (8)$$

and k_p is the wavenumber at which the initial energy spectrum is maximum. In this study, simulations with $s = 2$ and $s = 4$ were performed, corresponding to the initial energy spectra with a low wavenumber form proportional to either k^2 or k^4 .

Because the principal interest of this work was examination of the long-time evolution of rotating turbulence, it was necessary to use as large a value of k_p as possible in order that flow evolution not be adversely affected by the periodic boundary conditions used in the simulations; adverse affects occurring when the integral length scales of the flow become comparable to the box size. Another important consideration in these simulations was the aspect ratio of the computational domain.

Because of the rapid growth of turbulence length scales along the direction of the rotation axis, it was necessary to use a computational box which was longer along the rotation axis than in the other directions. Preliminary calculations of rotating turbulence on cubic domains had shown an adverse affect of periodicity because of the rapid integral scale growth along the rotation axis. Numerical experiments showed that it was necessary to use to a computational box which was four times larger along the rotation axis than in the directions orthogonal to the rotation vector. Four times as many collocation points were used in the vertical direction in order to avoid any effects of grid anisotropy at the smallest resolved scales.

Simulations were performed using resolutions of $96 \times 96 \times 384$ and $128 \times 128 \times 512$ collocation points. The governing equations (1) and (2) were solved using the pseudo-spectral method developed by Rogallo (1981). The statistical evolution of the flow using either resolution was essentially the same, and, therefore, only the results from the higher resolution computation are reported in this brief. The maximum physical wavenumber of the $128 \times 128 \times 512$ computations was 95 (for a computational domain having total volume of $8\pi^3$). The initial root-mean-square velocity fluctuation u_0 in (7) was equal to unity and $k_p = 75$. Following Chasnov (1993), the initial energy spectrum was set to zero for wavenumbers greater than 93 to allow the subgrid-scale eddy viscosity to build up from zero values. For each spectrum type, i.e., low wavenumber part proportional to k^2 or k^4 , simulations were performed with $\Omega = 0, 0.5, \text{ and } 1.0$.

2.2 Results

The instantaneous power-law exponent (i.e., the logarithmic time derivative) of the mean-square velocity fluctuation, $\langle \mathbf{u}^2 \rangle$, is shown in Figure 1 for each rotation rate and spectrum type used in the simulations. The time axis in Figure 1 and following figures has been made dimensionless using the eddy turnover time in the initial field

$$\tau(0) = L_u(0)/\langle \mathbf{u}^2 \rangle^{1/2} \quad (9)$$

where $L_u(t)$ is the velocity integral scale defined at time t as

$$L_u(t) = \frac{\pi}{2} \frac{\int_0^\infty k^{-1} E(k, t) dk}{\int_0^\infty E(k, t) dk}. \quad (10)$$

In isotropic turbulence, L_u is two-thirds the usual longitudinal integral scale measured in experiments (see also Chasnov 1993). Throughout this work, “ k^2 spectrum” refers to an initial energy spectrum $E(k)$ with low wavenumber part proportional to k^2 while “ k^4 spectrum” refers to an initial $E(k)$ with low wavenumbers proportional to k^4 . For both spectrum types, the characteristic effect of system rotation in reducing the decay rate of $\langle \mathbf{u}^2 \rangle$ is evident in Figure 1. Furthermore, it is also clear from the Figure that the value of the decay exponent for non-zero rotation rates at long times is independent of Ω , depending only on the form of the initial energy spectrum.

It is possible to predict the exponents in Figure 1 if one assumes that the asymptotic scaling of $\langle \mathbf{u}^2 \rangle$ is dependent on the form of $E(k)$ at low wavenumbers and

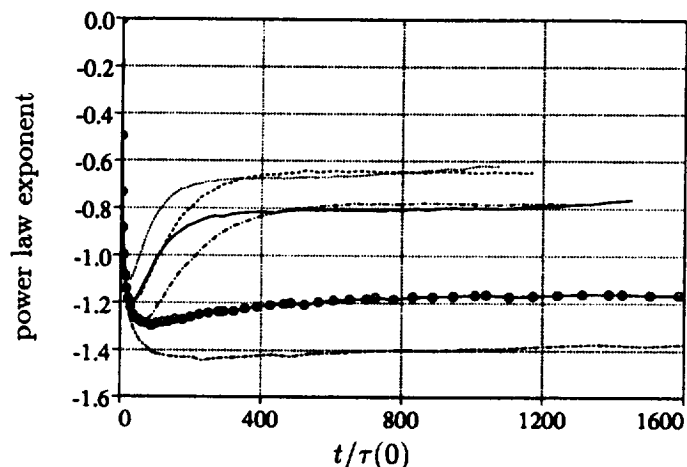


FIGURE 1. Time development of the power law exponent of $\langle \mathbf{u}^2 \rangle$ in rotating turbulence. \circ — \circ , $\Omega = 0$, k^2 spectrum; ----, $\Omega = 0.5$, k^2 spectrum; , $\Omega = 1.0$, k^2 spectrum; - · - ·, $\Omega = 0$, k^4 spectrum; — · —, $\Omega = 0.5$, k^4 spectrum; ———, $\Omega = 1.0$, k^4 spectrum.

independent of viscosity. For high Reynolds number turbulence, this is a reasonable assumption since the direct effect of viscosity occurs at much larger wavenumber magnitudes than those scales which contain most of the energy. Thus, it is possible to derive expressions for the asymptotic scaling of $\langle \mathbf{u}^2 \rangle$ using an expansion of the energy spectra near $k = 0$:

$$E(k) = 2\pi k^2(A_0 + A_2 k^2 + \dots) \quad (11)$$

where A_0, A_2, \dots are the Taylor series coefficients of the expansion. As shown by Batchelor & Proudman (1956), assuming that the velocity correlation tensor $\langle u_i(\mathbf{x})u_j(\mathbf{x} + \mathbf{r}) \rangle$ is analytic at $k = 0$ results in $A_0 = 0$ and a time-dependent value of A_2 . On the other hand, Saffman (1967) showed that it is also physically possible to create an isotropic turbulence with a non-zero value of A_0 , which is also invariant in time. As also shown by Chasnov (1993) the asymptotic scalings of $\langle \mathbf{u}^2 \rangle$ for these two cases are

$$\langle \mathbf{u}^2 \rangle \propto A_0^{2/5} t^{-6/5} \quad (k^2 \text{ spectrum}) \quad (12)$$

and

$$\langle \mathbf{u}^2 \rangle \propto A_2^{2/7} t^{-10/7} \quad (k^4 \text{ spectrum}). \quad (13)$$

It may be observed from Figure 1 that the agreement between the LES results and (12) and (13) is excellent for both spectrum types. An analysis similar to that leading to (12) and (13) may also be performed for flows having non-zero rotation rates. For non-zero Ω , the asymptotic scalings of $\langle \mathbf{u}^2 \rangle$ are predicted to be

$$\langle \mathbf{u}^2 \rangle \propto A_0^{2/5} t^{-3/5} \Omega^{3/5} \quad (k^2 \text{ spectrum}) \quad (14)$$

and

$$\langle \mathbf{u}^2 \rangle \propto A_2^{2/7} t^{-5/7} \Omega^{5/7} \quad (k^4 \text{ spectrum}). \quad (15)$$

For the k^2 spectrum, the value of the decay exponent from the rotating flows in the asymptotic region, approximately -0.64, is in very good agreement with (14). Similar agreement between the predicted value of the decay exponent, -5/7, and the measured values for the k^4 spectrum is also observed.

Evolution of the integral length scales are shown in Figures 2a and 2b. The vertical integral scale is defined as

$$L_v = \frac{1}{\langle \mathbf{u}^2 \rangle} \int \langle u_i(x, y, z) u_i(x, y, z + r) \rangle dr \quad (16)$$

while the horizontal integral scale is given by

$$L_h = \frac{1}{\langle \mathbf{u}^2 \rangle} \int \frac{\langle u_i(\mathbf{x}) u_i(\mathbf{x} + \mathbf{r}) \rangle}{2\pi r} d\mathbf{r}. \quad (17)$$

Figure 2 clearly shows the significantly greater growth in time of the vertical integral scales relative to their horizontal counterparts in rotating turbulence. Also shown in the Figure is the velocity integral scale, L_u , for $\Omega = 0$. It is evident from Figure 2 that the horizontal integral scales in the simulations with non-zero Ω are essentially independent of rotation rate and evolve similarly to the length scale from the non-rotating case.

The results in Figure 2 may be used to deduce *a posteriori* the asymptotic scaling laws of the integral scales. For the k^2 spectrum, dimensional arguments and the LES results in Figure 2a give the following dependence of the length scales on the invariant A_0 , t , and Ω

$$L_h \propto A_0^{1/5} t^{2/5} \quad (k^2 \text{ spectrum}), \quad (18)$$

i.e., no dependence of L_h on Ω . The appropriate scaling of the vertical length scales for the k^2 spectrum is

$$L_v \propto A_0^{1/5} t \Omega^{3/5} \quad (k^2 \text{ spectrum}) \quad (19)$$

since the long-time growth of L_v is observed from the LES results to be directly proportional to time. Similarly, dimensional arguments together with the results in Figure 2b can be used to deduce the length scale dependence on A_2 , t , and Ω for the k^4 spectrum:

$$L_h \propto A_2^{1/7} t^{2/7} \quad (k^4 \text{ spectrum}), \quad (20)$$

similar to the non-rotating case. For the vertical length scales

$$L_v \propto A_2^{1/7} t \Omega^{5/7} \quad (k^4 \text{ spectrum}). \quad (21)$$

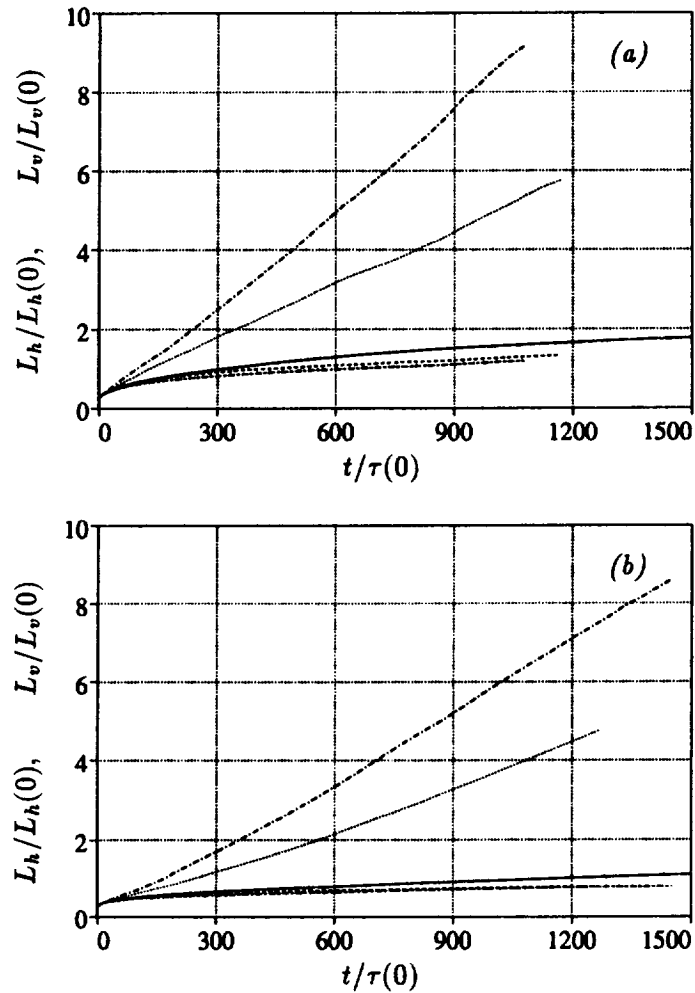


FIGURE 2. Time development of the integral length scales in rotating turbulence. (a) k^2 spectrum, (b) k^4 spectrum. —, L_u , $\Omega = 0$; ----, L_h , $\Omega = 0.5$; ·····, L_v , $\Omega = 0.5$; - - - - , L_h , $\Omega = 1.0$; - · - · , L_v , $\Omega = 1.0$.

As was the case for the simulations possessing a k^2 spectrum, long-time evolution of L_v in the simulations having a k^4 spectrum was also observed to be directly proportional to time.

As shown in Figures 2a and 2b, the evolution of the flow in the direction along the vertical axis is strongly enhanced relative to the horizontal directions. Rapid growth of the vertical length scales provides an indication of evolution towards a two-dimensional state. This can be more clearly seen through examination of the energy spectrum as a function of spatial wavenumber k as well as the cosine of the polar angle in wave space (schematically illustrated in Figure 3).

Shown in Figure 4a is the energy spectrum as a function of both k and $\cos \theta$ from a simulation with $\Omega = 0$ and possessing an initial spectrum with low wavenumber part

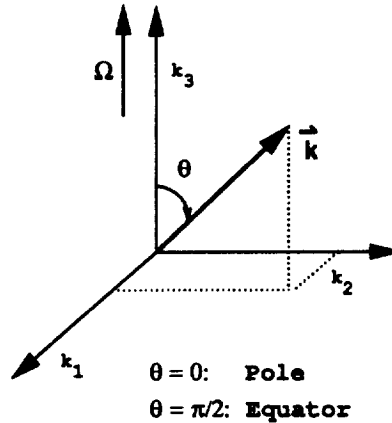


FIGURE 3. Wavenumber space showing rotation vector and polar angle θ . For simulations of rotating turbulence, the pole is defined as $\theta = 0$ ($\cos\theta = 1$); the equator as $\theta = \pi/2$ ($\cos\theta = 0$). Energy and transfer spectra are considered to be functions of both k and $\cos\theta$.

proportional to k^4 . It may be observed from the Figure that, as expected, the energy is essentially equi-partitioned with respect to $\cos\theta$. Plotted in Figure 4b is the energy spectrum from a simulation with $\Omega = 1$ (and k^4 spectrum). It is clear there is a marked concentration of energy in the equatorial plane, $\theta = \pi/2$; the Figure provides very strong evidence of the development of two-dimensional turbulence. This result is also in sharp contrast to the previous examinations of $E(k, \cos\theta)$ by Mansour *et al.* (1992) using direct numerical simulation. Mansour *et al.* found only a slight tendency for a concentration of energy near the equator. Because of viscous dissipation in their simulations, it was not possible for Mansour *et al.* to integrate the flow fields for long enough times in order to observe development of two-dimensional turbulence. It is important to emphasize that development of a two-dimensional state as demonstrated by Figure 4b cannot be captured by DNS because of viscous decay. LES circumvents this restriction and permits long enough integrations such that the non-linear interactions responsible for two-dimensionalization can occur.

Further evidence of the profound effect of rotation is contained in Figures 5a and 5b. Figure 5a is the transfer function, $T(k, \cos\theta)$, from a simulation with k^2 spectrum and $\Omega = 0$. The Figure shows the expected behavior, i.e., negative transfer at low wavenumbers and positive transfer at higher wavenumbers. It is also reasonably clear from Figure 5a that, as was the case with the energy spectrum, the transfer term is independent of θ . The transfer term from the simulation with a k^2 spectrum and $\Omega = 1.0$ is shown in Figure 5b. As is clear from the Figure, rotation has substantially altered the transfer spectrum. For values of $\cos\theta$ near 1 (the pole in k -space), the energy transfer is small for the low wavenumbers and zero at the higher wavenumbers. For $\cos\theta$ near 0 (the equator in k -space), the transfer term is actually *positive* at low wavenumbers, indicating a transfer of energy *into* these modes.

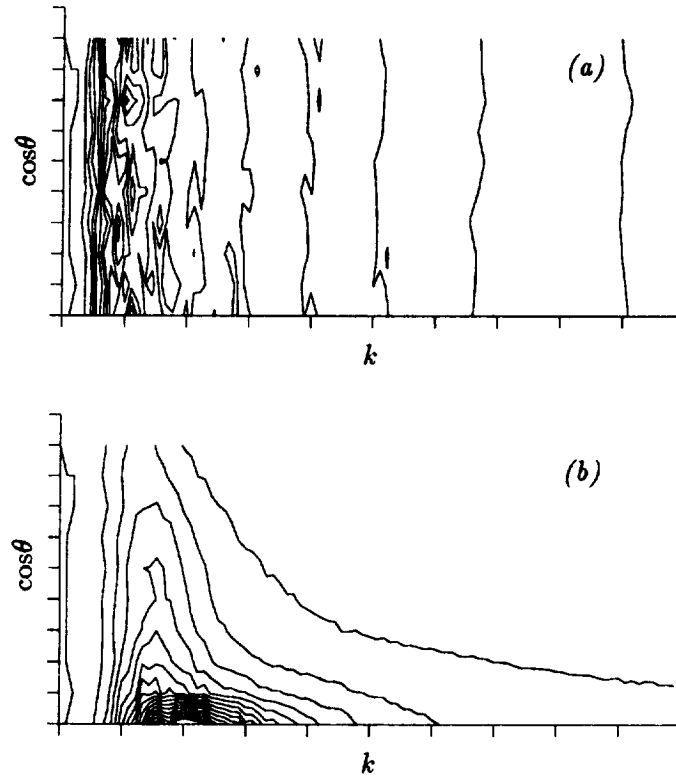


FIGURE 4. Energy spectrum as a function of wavenumber k and cosine of the polar angle θ ; spectrum obtained from LES with k^4 spectrum. (a) $\Omega = 0$ at $t/\tau(0) = 427$, (b) $\Omega = 1.0$ at $t/\tau(0) = 575$.

Time development of the two- and three-dimensional components of the kinetic energy are shown in Figures 6a and 6b for both spectrum types and each rotation rate. The two-dimensional component of the energy is obtained from Fourier modes in the plane $k_z = 0$ while the three-dimensional component is from Fourier modes with $k_z \neq 0$. The behavior is similar in both Figures and corroborates many of the aspects of the flows observed in the previous Figures. As expected, it may be observed that the decay of the energy is reduced with increasing rotation rates. More importantly, the Figures also show that for non-zero Ω the two-dimensional energy actually *increases* at later times in the flow evolution, consistent with Figure 5b showing a transfer of energy into the low wavenumber modes in the equatorial plane.

Figures 7a and 7b show the temporal evolution of the diagonal components of the anisotropy tensor of the Reynolds stress

$$b_{ij} = \frac{\langle u_i u_j \rangle}{\langle \mathbf{u}^2 \rangle} - \frac{\delta_{ij}}{3} \quad (22)$$

for each spectrum type and $\Omega = 0$ and 1.0. It is interesting to note that, while

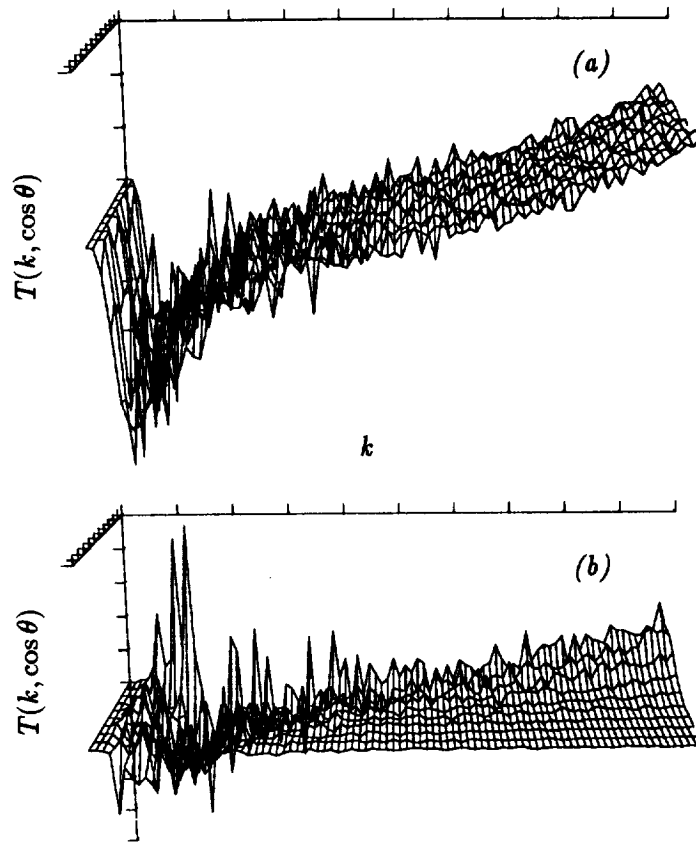


FIGURE 5. Transfer spectrum as a function of wavenumber k and cosine of the polar angle θ ; spectrum obtained from LES with k^2 spectrum. (a) $\Omega = 0$ at $t/\tau(0) = 725$, (b) $\Omega = 1.0$ at $t/\tau(0) = 552$.

the flow is becoming two-dimensional under the influence of system rotation, the distribution of kinetic energy amongst the three components shows little departure from isotropic values. As shown in the Figures, the vertical fluctuations are slightly enhanced by rotation relative to the fluctuations in the horizontal plane. The development of the diagonal components of the anisotropy tensor of the vorticity

$$v_{ij} = \frac{\langle \omega_i \omega_j \rangle}{\langle \omega^2 \rangle} - \frac{\delta_{ij}}{3} \quad (23)$$

is shown in Figure 8. In contrast to the Reynolds stress anisotropy, this Figure shows an enhancement of vertical vorticity relative to the horizontal components.

It is worthwhile to point out that recent work by Bartello *et al.* (1993) showed a much stronger departure from isotropy of the component energies in rotating turbulence. Bartello *et al.* used cubic domains to examine the long-time evolution of the flow and consequently the evolution of the component energies was adversely impacted. Based on their findings, Bartello *et al.* concluded that the long-time

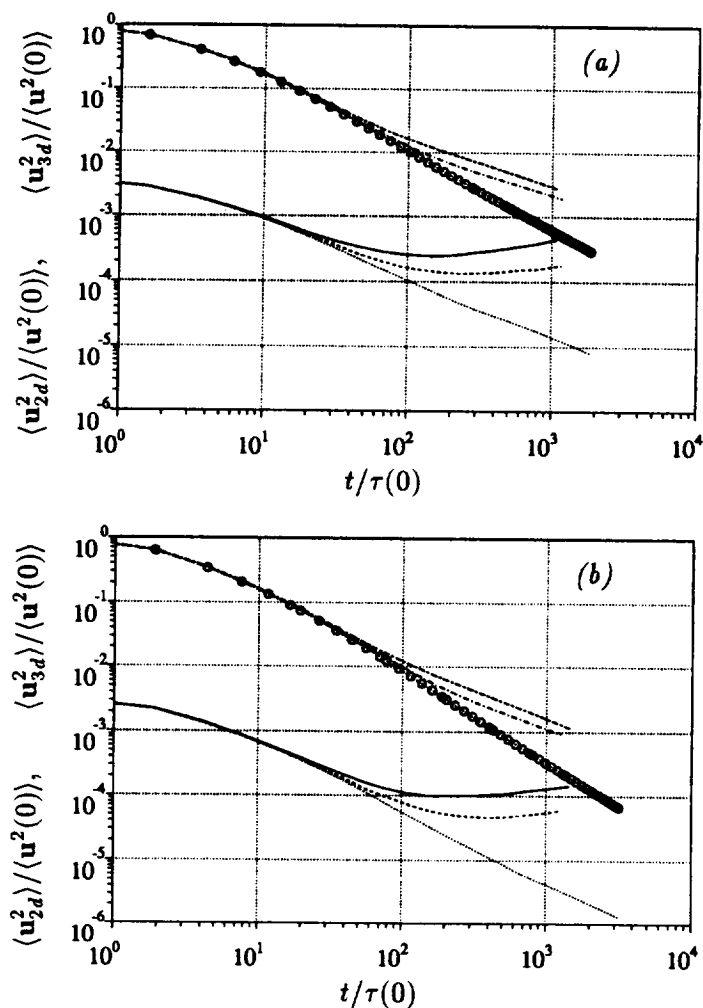


FIGURE 6. Evolution of two-dimensional and three-dimensional energy in LES. (a) k^2 spectrum, (b) k^4 spectrum. \cdots , 2D energy, $\Omega = 0$; $\circ\cdots\circ$, 3D energy, $\Omega = 0$; $----$, 2D energy, $\Omega = 0.5$; $---$, 3D energy, $\Omega = 0.5$; $—$, 2D energy, $\Omega = 1.0$; $----$, 3D energy, $\Omega = 1.0$.

state of homogeneous rotating turbulence was two-dimensional and two-component. However, it is clear from Figures 7 and 8 that the asymptotic state of homogeneous rotating turbulence is two-dimensional but *three*-component.

3. Future plans

LES results presented in this work demonstrated the existence of asymptotically self-similar states in rotating homogeneous turbulence. Additional investigations are planned to further corroborate this finding, e.g., examining the collapse of the spatial spectra under the appropriate scalings. Related to this issue are the particular scalings found in the present work. For example, the scaling laws for $\langle u^2 \rangle$

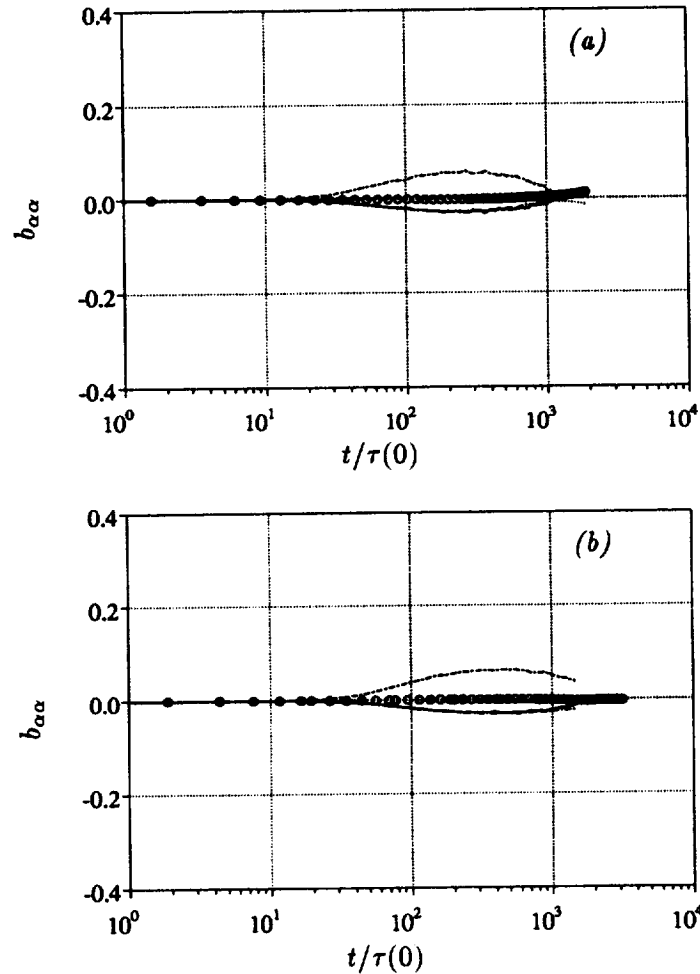


FIGURE 7. Evolution of Reynolds stress anisotropy tensor. (a) k^2 spectrum, (b) k^4 spectrum. Note that the curves for $\Omega = 0$ are essentially coincident and lie along the axis $b_{\alpha\alpha} = 0$. $\cdots\cdots$, b_{11} , $\Omega = 0$; $\circ\cdots\circ$, b_{22} , $\Omega = 0$; $\cdots\cdots$, b_{33} , $\Omega = 0$; --- , b_{11} , $\Omega = 1.0$; --- , b_{22} , $\Omega = 1.0$; --- , b_{33} , $\Omega = 1.0$.

in rotating turbulence (Equations 14 and 15) can be obtained using the transport equation for $\langle u^2 \rangle$ together with dimensional analysis. The scaling laws for the length scales, however, (Equations 18–21) rely on only dimensional analysis and a *posteriori* examination of LES results. Development of a more rigorous approach for predicting the length scale evolution observed in the present work would be desirable.

This study also showed the utility of large-eddy simulation. As shown in this work, development of an asymptotic state which is two-dimensional (but three-component) is very significant, much more so than in previous examinations of rotating turbulence using DNS. Given the encouraging results obtained to date, a

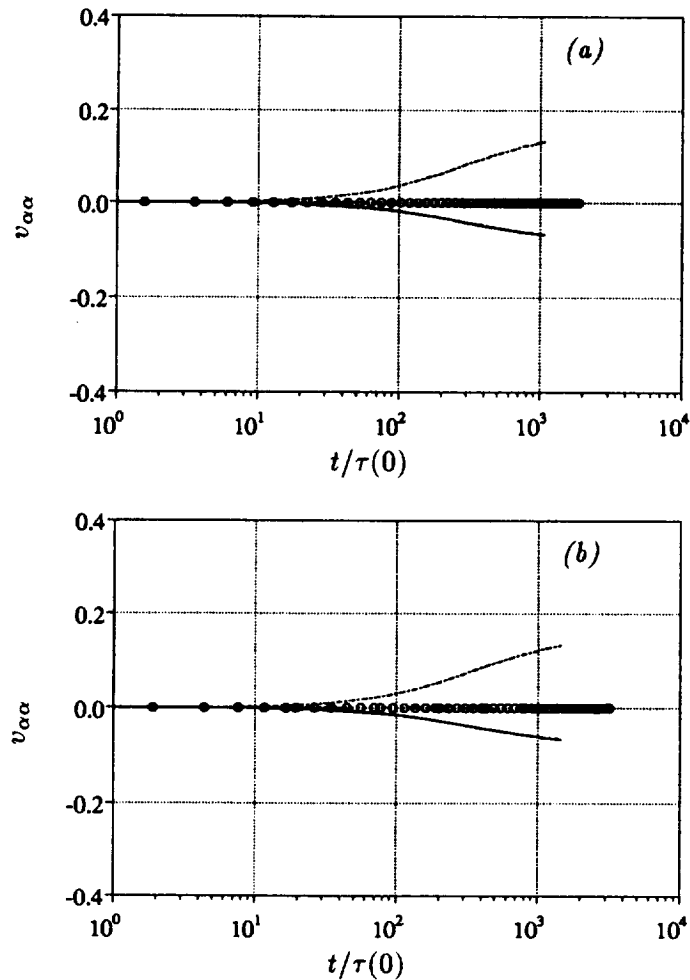


FIGURE 8. Evolution of vorticity anisotropy tensor. (a) k^2 spectrum, (b) k^4 spectrum. Note that the curves for $\Omega = 0$ are essentially coincident and lie along the axis $v_{\alpha\alpha} = 0$. $\cdots\cdots$, v_{11} , $\Omega = 0$; $\circ\cdots\circ$, v_{22} , $\Omega = 0$; $-\cdots-$, v_{33} , $\Omega = 0$; $-\cdot-\cdot-$, v_{11} , $\Omega = 1.0$; $-\cdot-\cdot-$, v_{22} , $\Omega = 1.0$; $-\cdot-\cdot-$, v_{33} , $\Omega = 1.0$.

likely extension of this work will be use of the LES database for developing a high Reynolds number extension of the $k-\varepsilon$ model for rotating flows.

Acknowledgements

Financial support of the first author provided by a NASA-ASEE Summer Faculty Fellowship is gratefully acknowledged. The authors are also grateful to Dr. Robert Rogallo for the use of his code and the support of Dr. Alan Wray for his assistance with the Vectoral language. The simulations were performed on the Cray C90 at the NASA Ames Research Center.

REFERENCES

- BARDINA, J., FERZIGER, J. H. & ROGALLO, R. S. 1985 Effect of rotation on isotropic turbulence: computation and modeling. *J. Fluid Mech.* **154**, 321-336.
- BARTELLO, P., METAIS, O. & LESIEUR, M. 1993 Coherent structures in rotating three-dimensional turbulence. *J. Fluid Mech.* In press.
- BATCHELOR, G. K. & PROUDMAN, I. 1956 The large-scale structure of homogeneous turbulence. *Phil. Trans. Roy. Soc.* **248**, 369.
- CHASNOV, J. R. 1993 Similarity states of passive scalar transport in isotropic turbulence. *Phys. Fluids A*. in press.
- CHOLLET, J. P. & LESIEUR, M. 1981 Parameterization of small scales of three-dimensional isotropic turbulence utilizing spectral closures. *J. Atmos. Sci.* **38**, 2747.
- JACQUIN, L., LEUCHTER, O., CAMBON, C. & MATHIEU, J. 1990 Homogeneous turbulence in the presence of rotation. *J. Fluid Mech.* **220**, 1-52.
- GREENSPAN, H. P. 1968 *The Theory of Rotating Fluids*. Cambridge University Press.
- MANSOUR, N. N., CAMBON, C. & SPEZIALE, C. G. 1991 Single point modeling of initially isotropic turbulence under uniform rotation. *Annual Research Briefs - 1991*, NASA-Stanford Center for Turbulence Research.
- MANSOUR, N. N., CAMBON, C. & SPEZIALE, C. G. 1992 Theoretical and computational study of rotating isotropic turbulence. *Studies in Turbulence*, edited by T. B. Gatski, S. Sarkar & C. G. Speziale, (Springer-Verlag).
- ROGALLO, R. S. 1981 Numerical experiments in homogeneous turbulence. *NASA TM 81315*.
- SAFFMAN, P. G. 1967 The large-scale structure of homogeneous turbulence. *J. Fluid Mech.* **27**, 581.
- SPEZIALE, C. G., MANSOUR, N. N. & ROGALLO, R. S. 1987 The decay of isotropic turbulence in a rapidly rotating frame. *Proc. of the 1987 Summer Program, Report CTR-S87*, NASA-Stanford Center for Turbulence Research.
- TRAUGOTT, S. C. 1958 Influence of solid-body rotation on screen-produced turbulence. *NACA Tech. Note 4135*.
- VEERAVALLI, S. V. 1991 An experimental study of the effects of rapid rotation on turbulence. *Annual Research Briefs - 1991*, NASA-Stanford Center for Turbulence Research.